COMMUNICATION

TEMPO Coordination and Reactivity in Group 6; Pseudo-Pentagonal Planar (η^2-TEMPO)$_2$CrX (X = Cl, TEMPO)

Ann K. Kayser,[a] Peter T. Wolczanski*,[a] Thomas R. Cundari,[b] Melissa M. Bollmeyer,[a] Kyle M. Lancaster,[a] and Samantha N. MacMillan[a]

[a] Dept. of Chemistry and Chemical Biology Baker Laboratory, Cornell University, Ithaca, NY, USA, 14853; ptw2@cornell.edu
[b]Dept. of Chemistry, CasCam, University of North Texas, TX, USA, 76201

Supplementary Information

Table of Contents **p**

I. Experimental
A. General Experimental **S2**
B. Procedures **S2**
C. X-ray Crystallographic Data **S3**
D. Computations **S4**
E. TD-DFT Computed Spectra **S7**
II. References **S9**

I. Experimental

A. General Experimental. All manipulations were performed using either glovebox or high vacuum line techniques. All glassware was oven-dried for 30 min and evacuated while hot in either a glovebox chamber or on a high vacuum line. THF and diethyl ether were distilled under nitrogen from purple sodium benzophenone ketyl and vacuum transferred from the same prior to use. Hydrocarbon solvents were treated in the same manner with the addition of 1-2 mL/L tetraglyme. Benzene-d_6 was dried over sodium, vacuum transferred and stored over activated 4Å molecular sieves. THF-d_8 was dried over sodium and stored over purple sodium benzophenone ketyl. DMSO-d_6 was dried over 4Å molecular sieves for 18 h, distilled, and stored over 4Å molecular sieves.

[TEMPO]Na was made by refluxing the free radical with equimolar amounts of sodium in hexanes overnight, and filtered to collect the product.[1] $CrCl_2(THF)_2$ was prepared by Soxhlet extraction for 5 d.[2] The solid was filtered, and washed with THF and hexanes.

NMR spectra were acquired using Mercury 300 MHz or Bruker AV III HD 500 MHz (equipped with a 5 mm BBO Prodigy cryoprobe) spectrometers. Chemical shifts are reported relative to benzene-d_6 (^{1}H δ 7.16; ^{13}C{^{1}H} δ 128.06) or THF-d_8 (^{1}H d 3.58; ^{13}C{^{1}H} d 67.57). UV-Vis spectra were acquired using a Cary 60 UV-Vis spectrometer with standard 1 cm quartz cuvettes.

B. Procedures. 1. (η^2-O,N-TEMPO)$_2$CrCl (1). To a 50 mL round-bottom flask was added $CrCl_2(THF)_2$ (100 mg, 0.374 mmol), TEMPO (60 mg, 0.374 mmol), and [TEMPO]Na (68 mg, 0.379 mmol). The flask was cooled to -78 °C, and Et_2O (30 mL) was distilled into the vessel. The purple solution was warmed to 25 °C and stirred for 16-24 h, and filtered. The filter cake was washed with Et_2O (3 x 5 mL), and the combined filtrates were concentrated (~10 mL), cooled to -78 °C, and stirred for 30 min. The solution was filtered, and the product was collected as lavender crystals (100 mg, 67%). Single crystals suitable for X-ray diffraction were grown by slow evaporation of a concentrated Et_2O solution at -35 °C. ^{1}H NMR (300 MHz, benzene-d_6) d 0.04, 0.47, 14.78, 16.08. μ_{eff} (Evans') = 3.7 μ_B.

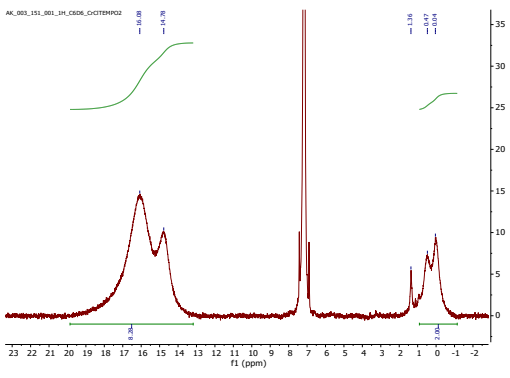

Fig. S1. ^{1}H NMR spectrum of (η^2-O,N-TEMPO)$_2$CrCl (**1**) in C_6D_6.

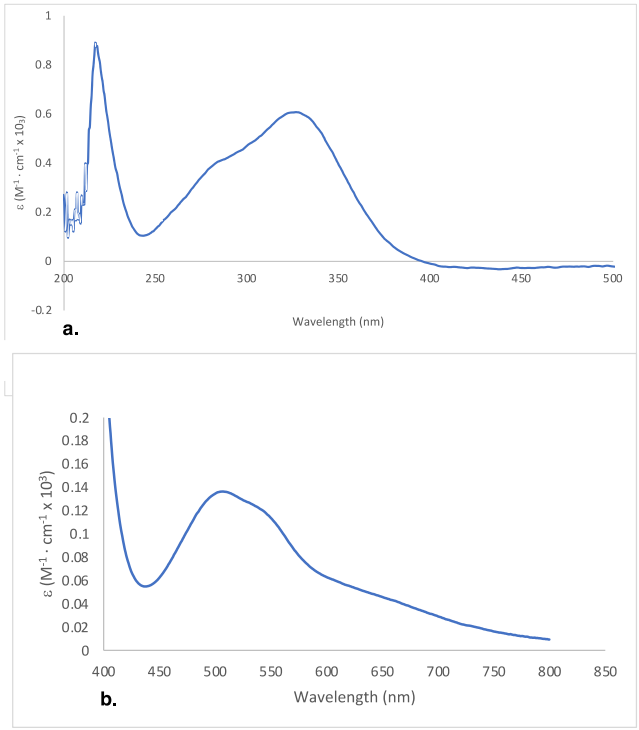

Fig. S2. UV-vis spectrum of (η^2-O,N-TEMPO)$_2$CrCl (**1**) in Et_2O: **a.** $\lambda(\varepsilon)$ ~ 325 nm (604 $M^{-1}cm^{-1}$); $\lambda(\varepsilon)$ ~ 285 nm (406 $M^{-1}cm^{-1}$); **b.** $\lambda(\varepsilon)$~ 640 nm (50 $M^{-1}cm^{-1}$); $\lambda(\varepsilon)$ ~ 540 nm (125 $M^{-1}cm^{-1}$), $\lambda(\varepsilon)$ ~ 510 nm (140 $M^{-1}cm^{-1}$).

2. (η^2-O,N-TEMPO)$_2$Cr(TEMPO) (2). To a 25 mL round-bottom flask was added $CrCl(TEMPO)_2$ (50 mg, 125 mmol) and [TEMPO]Na (23 mg, 0.125 mmol). The flask was cooled to -78 °C, and Et_2O (15 mL) was distilled into the vessel. The golden solution was warmed to -35 °C and stirred for 16-24 h at which point it was warmed to just ~20 °C and filtered. The solution was concentrated, cooled to -78 °C, stirred for 30 min, and filtered to afford purple-yellow dichroic crystals (35 mgs, 53 %). Single crystals suitable for X-ray diffraction were grown by slow evaporation of a dilute Et_2O solution at -35 °C. The solid product is stable in at -35 °C for several weeks. A solution of the product at 23 °C will decompose into TMP-containing organics and CrO_n; k = 0.022, $t_{1/2}$ = 31.7 h. ^{1}H NMR (300 MHz, benzene-d_6) δ -4.09, -1.78, 2.57, 10.24, 20.95, 52.09. μ_{eff} (Evans') = 3.6 μ_B.

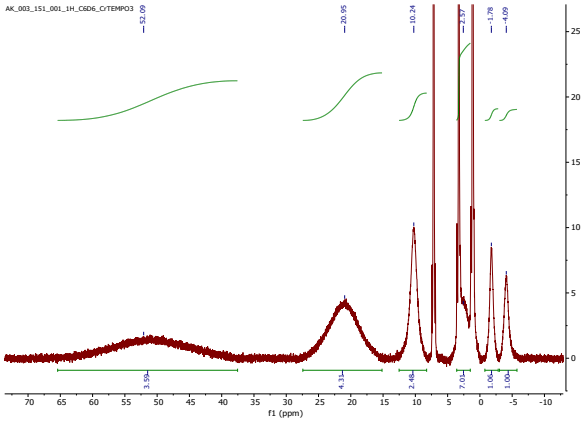

Fig. S3. ^{1}H NMR spectrum of (η^2-O,N-TEMPO)$_2$Cr(TEMPO) (**2**) in C_6D_6.

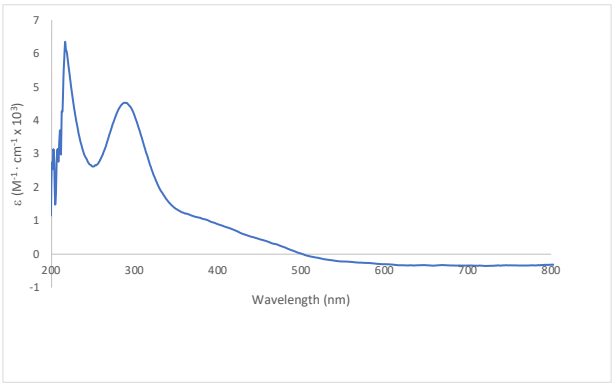

Fig. S4. UV-vis spectrum of (η^2-O,N-TEMPO)$_2$Cr(TEMPO) (**2**) in Et_2O: λ(ε)~ 466 (358); λ(ε) ~ 381 (1060). λ(ε) ~ 289 (451).

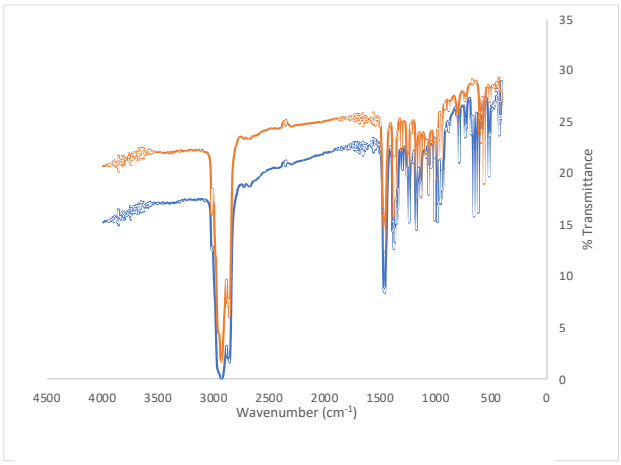

Fig. S5. IR spectra of (η^2-O,N-TEMPO)$_2$CrCl (**1**) (orange) and (h^2-O,N-TEMPO)$_2$Cr(TEMPO) (**2**) (blue); nujol mull.

3. (η^2-O,N-TEMPO)$_2$MoO$_2$. To a 50 mL round bottom flask was added $MoCl_3(THF)_3$ (100 mg, 0.238 mmol), TEMPO (1 equiv, 30mg, 0.238 mmol), and [TEMPO]Na (3 equiv, 129 mg, 0.717 mmol). The flask was cooled to -78°C, and Et_2O (40-50 mL) was distilled into the vessel (40-50 mL). The yellow solution was warmed to 23 °C, stirred for 24-36 h, and filtered. The reaction was concentrated to ~10 mL and cooled to -78 °C to precipitate yellow microcrystals, which were collected via filtration (31 mg, 30%). Single crystals suitable for XRD were grown by slow evaporation of an Et_2O solution at -35°C. ^{1}H NMR (500 MHz, benzene-d_6) δ 0.85 (s, 3H, CH_3), 0.95 (s, 3H, CH_3), 1.07(s, 3H, CH_3), 1.21 (3H, CH_3), 1.24 (m, 2H, CH_2), 1.30 (m, 4H, CH_2), 1.37 (m, 4H, CH_2) 1.51 (m, 2H, CH_2), 1.52 (s, 6H, CH_3), 1.64 (s, 6H, CH_3). ^{13}C {^{1}H} NMR (126 MHz, benzene-d_6) δ 16.89 (CH_2), 22.82 (CH_3), 23.49 (CH_3), 27.53 (CH_3) 30.24 (CH_2), 32.10 (CH_3), 32.15 (CH_3), 33.14 (CH_3), 37.94 (CH_2), 39.26/39.25 (2C, CH_2), 64.31 ($C(CH_3)_2$), 67.46 ($C(CH_3)_2$).

C. Crystallographic Data. 4. (η^2-O,N-TEMPO)$_2$CrCl (1) (0.24 x 0.21 x 0.06 mm^3)**:** $C_{18}H_{36}ClCrN_2O_2$, M = 399.94, T = 100.0(5) K, λ = 1.54184 Å, orthorhombic, Pbca, a = 10.198910(10), b = 14.66290(10), c = 27.4065(2) Å, α = β = γ = 90°, V = 4098.20(6) Å^3, Z = 8, ρ (calcd) = 1.296 g/cm^3, abs. coeff. = 5.883 mm^{-1}, 30256 reflections, 4352 independent, R_{int} = 0.0390, Gaussian abs. correc., $R_1(I > 2\sigma I)$ = 0.0271, wR_2 = 0.0708, R_1(all data) = 0.0292, wR_2 = 0.0721, GOF = 1.062, CCDC-2154283.

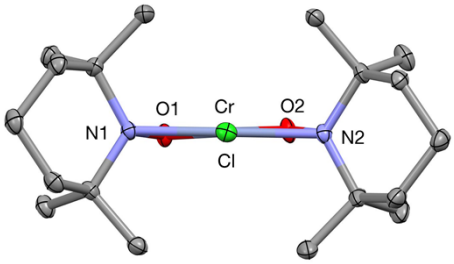

Figure S6. Molecular view of (η^2-O,N-TEMPO)$_2$CrCl (**1**) showing planarity.

5. (η^2-O,N-TEMPO)$_2$Cr(TEMPO) (2). (0.25 x 0.17 x 0.15 mm^3)**:** $C_{27}H_{54}CrN_3O_3$, M = 520.73, T = 99.9(3) K, λ = 1.54184 Å, triclinic, P1bar, a = 9.75440(10), b = 10.23250(10), c = 15.2956(2) Å, α = 100.0300(10)°, β = 93.7780(10)°, γ = 106.5100(10)°, V = 1430.56(3) Å^3, Z = 2, ρ (calcd) = 1.209 g/cm^3, abs. coeff. = 3.522 mm^{-1}, 30784 reflections, 5171 independent, R_{int} = 0.0667, Gaussian abs. correc., $R_1(I > 2\sigma I)$ = 0.0487, wR_2 = 0.1265, R_1(all data) = 0.0505, wR_2 = 0.1285, GOF = 1.061, CCDC-2154281.

6. (η^2-O,N-TEMPO)$_2$MoO$_2$ (3). (0.23 x 0.15 x 0.10 mm^3)**:** $C_{18}H_{36}MoN_2O_4$, M = 440.43, T = 99.9(4) K, λ = 0.71073 Å, monoclinic, P2$_1$/n, a = 12.0580(6), b = 15.6515(5), c = 12.1533(5) Å, β = 118.845(6)°, V = 2009.06(18) Å^3, Z = 4, ρ (calcd) = 1.456 g/cm^3, abs. coeff. = 0.667 mm^{-1}, 12030 reflections, 3960 independent, R_{int} = 0.0319, Gaussian abs. correc., $R_1(I > 2\sigma I)$ = 0.0476, wR_2 = 0.1057, R_1(all data) = 0.0533, wR_2 = 0.1095, GOF = 1.132, CCDC-2154282.

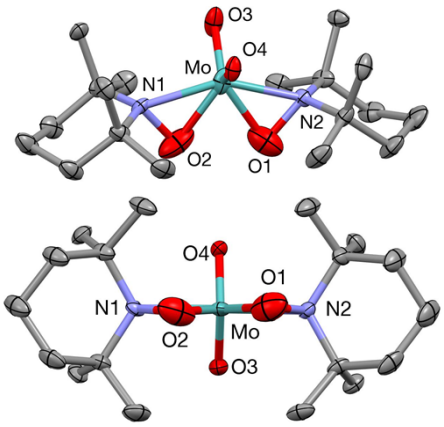

Figure S7. Molecular views of (h^2-O,N-TEMPO)$_2$MoO$_2$ (**3**). Selected distances (Å) and angles (°): MoO1, 1.993(5); MoO2, 1.988(5); MoO3, 1.717(3); MoO4, 1.710(3); MoN1, 2.139(3); MoN2, 2.128(3); O1N2, 1.443(5); O2N1, 1.425(4); O1MoO2, 68.17(16); O1MoO3, 121.23(15); O1MoO4, 115.91(15); O1MoN1, 108.23(14); O1MoN2, 40.82(13); O2MoO3, 117.74(15); O2MoO4, 118.86(14); O2MoN1, 40.20(13); O2MoN2, 108.82(13); O3MoO4, 109.83(14); O3MoN1, 99.25(12); O3MoN2, 98.66(12); O4MoN1, 98.31(11); O4MoN2, 99.12(11); Mo N1MoN2, 149.00(11); MoN1O2, 64.2(2); MoN2O1, 64.6(2); MoO1N2, 74.6(2); MoO2N1, 75.6(2).

Note (η^2-O,N-TEMPO)$_2$MoO$_2$ (**3**) crystallizes in a different space group (P2$_1$/n) than the structure previously reported (Pca2$_1$),[3] but the metric parameters and geometry appear to be the same. Note

that the NMR spectra of **3** intimate different TEMPO units, hence there may be a preferred unsymmetric conformer or different geometry in solution.

D. Computational Information. 1. Methods. Density functional theory simulations employed the Gaussian16 code,[4] and the wB97xD[5] functional in conjunction with the def2-tzvpp[6] basis set. Geometry optimizations of **1** and **2** were initiated from the crystal coordinates after normalizing the C–H bond lengths, and utilized an unrestricted Kohn-Sham formalism. Spin contamination was minimal with calculated $<S^2>$ expectation values of 3.85 and 3.82 for **1** and **2**, respectively. Vibrational frequencies were obtained to confirm the optimized structures as local minima.

To probe the energetics of the κ^1-O to η^2-N,O transformation, first one and then both η^2-TEMPO ligands were constrained to the 126.0° Cr-O-N angle computed for the κ^1-O-TEMPO ligand in fully optimized complex **2** (*vide supra*). Note that upon release of the constraints, geometry optimization led to structures essentially identical to fully optimized **2**.

Orbitals for **2** were plotted at the DFT optimized geometries using (a) restricted open-shell DFT, (b) unrestricted DFT, and (c) complete active space SCF (CASSCF) methods. For (a) and (b), the Gaussian16 code was used and for (c) the GAMESS[7] code and a 6-31G(d) basis set were employed. All approaches led to the same conclusion, *i.e.*, that the subject complexes are best viewed as high-spin, Cr(III) complexes with anionic TEMPO ligands, thus corroborating the metric analyses put forth in the manuscript.

2. Optimized Geometries. The optimized geometries in Figs. S8 and S9 corroborate the ground state quartet experimental structures of $(\eta^2$-O,N-TEMPO$)_2$CrCl (**1**) and $(\eta^2$-O,N-TEMPO$)_2$Cr(TEMPO) (**2**).

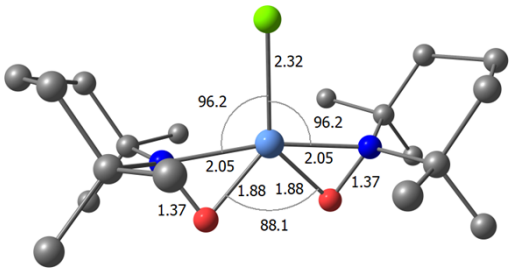

Figure S8. wB97xD/def2-tzvpp optimized geometry of $(\eta^2$-O,N-TEMPO$)_2$CrCl (**1**): bond distances are in Å; bond angles in degrees (°); geometry optimization was initiated from crystal structure with normalized hydrogen positions.

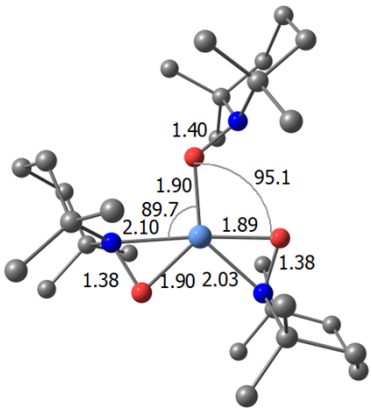

Figure S9. wB97xD/def2-tzvpp optimized geometry of $(\eta^2$-O,N-TEMPO$)_2$Cr(TEMPO) (**2**): bond distances are in Å; bond angles in degrees (°); geometry optimization was initiated from crystal structure with normalized hydrogen positions. The κ^1-TEMPO Cr-O-N angle is 126.0°.

3. Complete Active Space Orbitals SCF (CASSCF) Orbitals of (h^2-O,N-TEMPO)$_2$Cr(TEMPO) (2). Selected natural orbitals with calculated occupation numbers (in e^-) are given in Fig. S10.

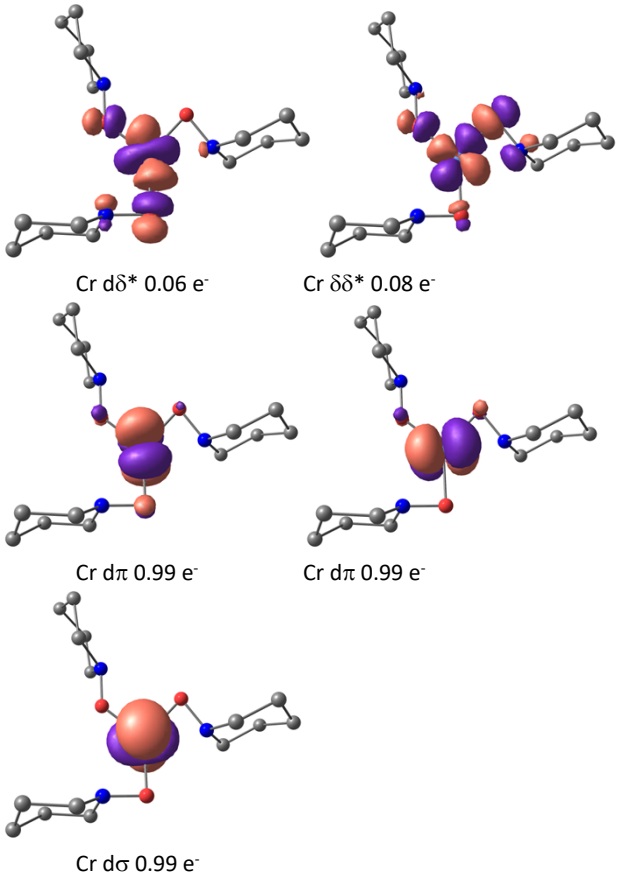

Figure S10. CASSCF (14 orb., 11 e^- active space) and 6-31G(d) basis set for $(\eta^2$-O,N-TEMPO$)_2$Cr(TEMPO) (**2**) Selected (ligand field) natural orbitals are shown and their character noted.

3. Unrestricted wB97xD/def2-tzvpp Orbitals for (η^2-O,N-

TEMPO)$_2$Cr(TEMPO) (2). A table (Table S1) and figures (Fig. S11 and S12) of unrestricted alpha and beta orbitals are given below.

Table 1. Unrestricted wB97xD/def2-tzvpp orbital energies (eV) for (η^2-O,N-TEMPO)$_2$Cr(TEMPO) (**2**).

Orbital #	alpha e	beta
133	-10.44	-10.21
134	-10.24	-10.21
135	-10.24	-9.88
136	-9-98	-9.79
137	-9.91	-9.52
138	-9.60	-8.97
139	-8.68	-8.62
140	-8.43	-8.32
141	-8.26	-6.63 [a]
142	-8.07	1.52 [b]
143	-7.69	2.32
144 [c]	-6.51	2.57
145 [d]	0.77	2.64
146	1.45	2.69
147	2.57	2.85
148	2.84	3.08
149	3.07	3.15

[a]b HOMO. [b]b LUMO. [c]a HOMO. [d]a LUMO.

The relevant alpha orbitals shown in Fig. S11 (T = TEMPO), and those beta orbitals in Fig. S12 are correlated with the orbital #'s and energies in Table S1.

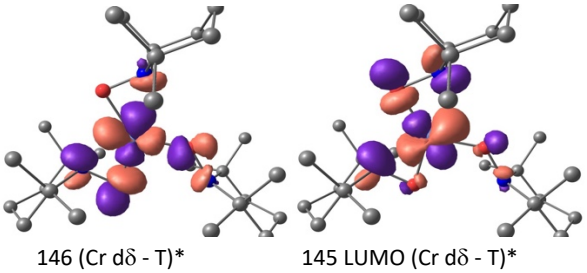

146 (Cr dδ - T)* 145 LUMO (Cr dδ - T)*

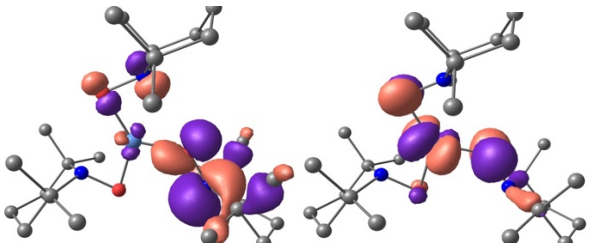

144 HOMO (T NO π)* 143 (Cr dπ + O pπ)

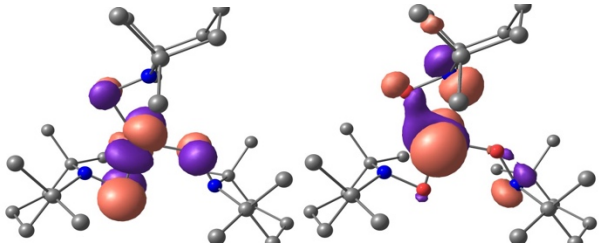

142 (Cr dπ + O pπ) 141 (Cr dσ)

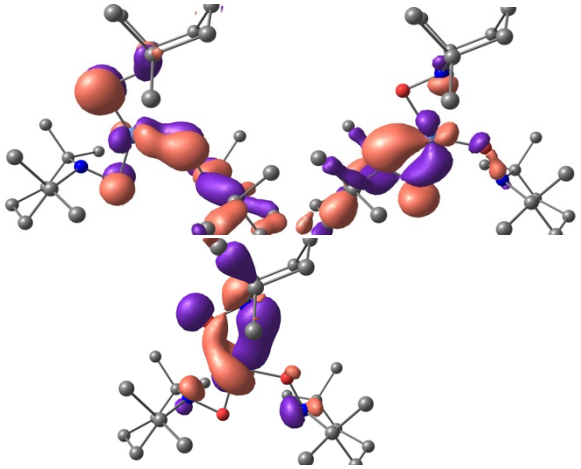

138-140 (Cr dπ + NO pπ*)

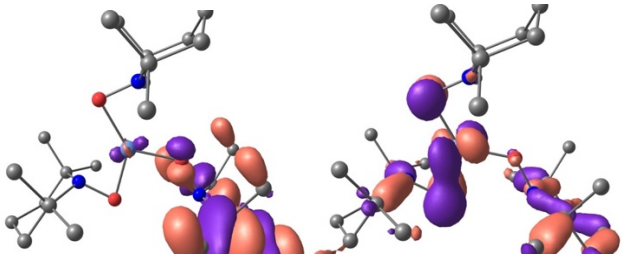

137 TEMPO 136 (Cr dπ + O pπ)

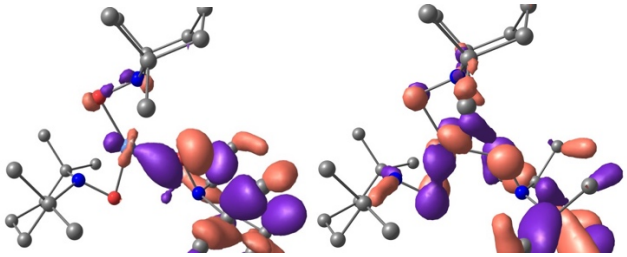

135 TEMPO 134 (Cr dp + O pπ)

Figure S11. Unrestricted wB97xD/def2-tzvpp alpha orbitals for (η^2-O,N-TEMPO)$_2$Cr(TEMPO) (**2**).

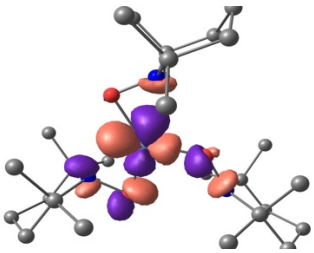

149 (Cr dδ) 147-148 diffuse

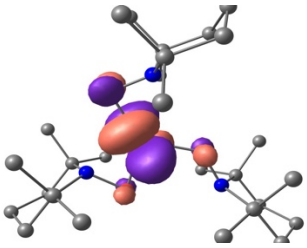

146 (Cr dπ) 145 diffuse

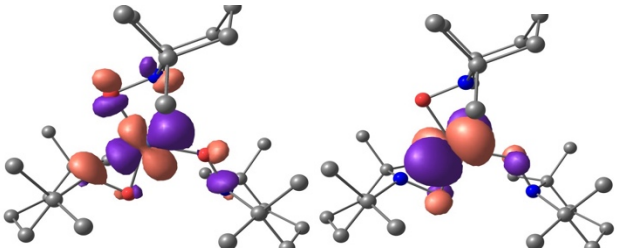

144 (Cr dδ) 143 (Cr dπ)

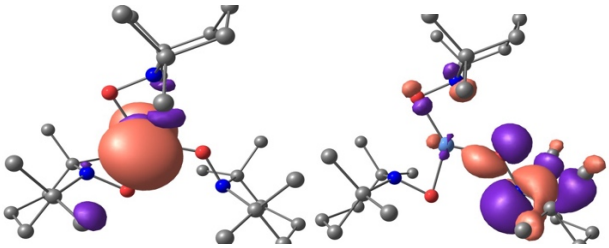

142 LUMO (Cr dσ) 141 HOMO (TEMPO NO π*)

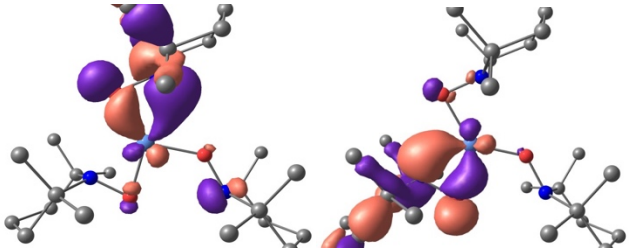

140 (TEMPO NO π*) 139 (TEMPO NO π*)

136-138 (TEMPO O π)

Figure S12. Unrestricted wB97xD/def2-tzvpp beta orbitals for (η^2-O,N-TEMPO)$_2$Cr(TEMPO) (**2**).

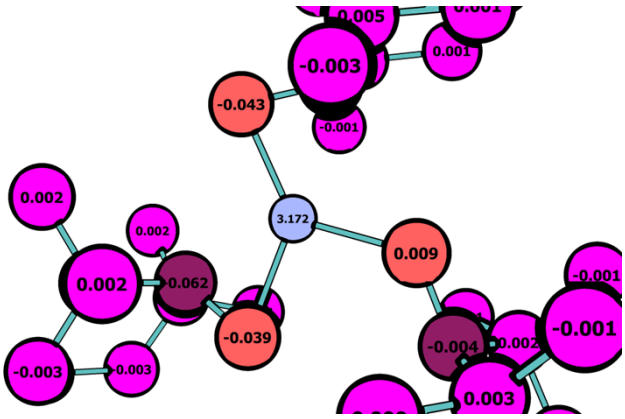

Figure S13. Calculated spin densities for the core atoms of (η^2-O,N-TEMPO)$_2$Cr(TEMPO) (**2**).

E. TD-DFT Computed spectra.

a.

b.

Figure S14. ωB97xD/def2-tzvpp computed TDDFT spectrum of (η^2-O,N-TEMPO)$_2$CrCl (**1**): **a**) 200-780 nm; **b)** blow-up of 400-800 nm region. Peak values are reported in nm.

a.

b.

Figure S15. ωB97xD/def2-tzvpp computed TDDFT spectrum of (η^2-O,N- TEMPO)$_2$Cr(TEMPO) (**2**): **a**) 200-780 nm; **b**) blow-up of 400-800 nm region. Peak values are reported in nm.

Table S2. TD-DFT calculated lambda maxima and oscillator strengths of (η^2-O,N-TEMPO)$_2$CrCl (**1**) and (η^2-O,N-TEMPO)$_2$Cr(TEMPO) (**2**).

(η^2-O,N-TEMPO)$_2$CrCl (**1**)		(η^2-O,N-TEMPO)$_2$Cr(TEMPO) (**2**)	
λ (nm)	**f**	**λ (nm)**	**f**
662.39	0.0001	758.65	0.0001
628.02	0	662.72	0.0002
598.29	0.0001	605.89	0.0004
525.62	0.0003	503.4	0.0001
494.72	0.0002	481.94	0.0002
486.41	0.0017	468.19	0.0033
337.89	0.1235	384.7	0.0219
308.02	0.006	342.46	0.0233
291.97	0.0007	319.75	0.0031
286.92	0.017	301.51	0.0075
245.87	0.0016	297.35	0.093
242.82	0.0022	285.86	0.0039
237.42	0	267.39	0.0004
234.53	0.0002	265.5	0.0053
231.27	0	256.27	0.0119
231.02	0.0006	247.76	0.0022
225.16	0.0001	246.07	0.0005
220.36	0.0002	236.74	0.0002
217.22	0.0055	233.81	0.0016
215.65	0.0004	232.78	0.0012

II. References

1 L. Balloch, A. M. Drummond, P. Garcia-Alvarez, D. V. Graham, A. R. Kennedy, J. Klett, R. E. Mulvey, C. T. O'Hara, P. J. A. Rodger, and I. D. Rushworth, *Inorg. Chem.*, 2009, **48**, 6934-6944.

2 R. J. Kern, *Inorg. Nucl. Chem.*, 1962, **24**, 1105-1109.

3 P. Jaitner, W. Huber, A. Gieren, and H. Betz, *Z. anorg. allg. Chem.*, 1986, **538**, 53-60.

4 M. J. Frisch, G. W. Trucks, H. B. Schlegel, G. E. Scuseria, M. A. Robb, J. R. Cheeseman, G. Scalmani, V. Barone, G. A. Petersson, and H. Nakatsuji, *et al. Gaussian 16, Revision A.03*; Gaussian, Inc.: Wallingford, CT, USA, 2016.

5 J.-D. Chai and M. Head-Gordon, *Phys. Chem. Chem. Phys.*, 2008, **10**, 6615–6620.

6 A. Hellweg and D. Rappoport, *Phys. Chem. Chem. Phys.*, 2015, **17**, 1010–1017.

7 M. Schmidt, K. K. Baldridge, J. A. Boatz, S. T. Elbert, M. S. Gordon, J. H. Jensen, S. Koseki, N. Matsunaga, K. A. Nguyen, S. Su, T. L. Windus, M. Dupuis, J. A. Montgomery, *J. Comput. Chem.*, 1993, **14**, 1347-136.